JOURNAL OF BACTERIOLOGY, June 2002, p. 2931–2939 Vol. 184, No. 11
0021-9193/02/$04.00+0 DOI: 10.1128/JB.184.11.2931–2939.2002

An Iron-Binding Protein, Dpr, from *Streptococcus mutans* Prevents Iron-Dependent Hydroxyl Radical Formation In Vitro

Yuji Yamamoto,[1] Leslie B. Poole,[2] Roy R. Hantgan,[2] and Yoshiyuki Kamio[1]*

Laboratory of Applied Microbiology, Department of Molecular and Cell Biology, Graduate School of Agricultural Science, Tohoku University, Amamiya-machi, Aoba-ku, Sendai 981-8555, Japan,[1] and Department of Biochemistry, Wake Forest University Medical School, Winston-Salem, North Carolina 27157[2]

Received 5 October 2001/Accepted 18 February 2002

The *dpr* gene is an antioxidant gene which was isolated from the *Streptococcus mutans* chromosome by its ability to complement an alkyl hydroperoxide reductase-deficient mutant of *Escherichia coli*, and it was proven to play an indispensable role in oxygen tolerance in *S. mutans*. Here, we purified the 20-kDa *dpr* gene product, Dpr, from a crude extract of *S. mutans* as an iron-binding protein and found that Dpr formed a spherical oligomer about 9 nm in diameter. Molecular weight determinations of Dpr in solution by analytical ultracentrifugation and light-scattering analyses gave values of 223,000 to 292,000, consistent with a subunit composition of 11.5 to 15 subunits per molecule. The purified Dpr contained iron and zinc atoms and had an ability to incorporate up to 480 iron and 11.2 zinc atoms per molecule. Unlike *E. coli* Dps and two other members of the Dps family, Dpr was unable to bind DNA. One hundred nanomolar Dpr prevented by more than 90% the formation of hydroxyl radical generated by 10 μM iron(II) salt in vitro. The data shown in this study indicate that Dpr may act as a ferritin-like iron-binding protein in *S. mutans* and may allow this catalase- and heme-peroxidase-deficient bacterium to grow under air by limiting the iron-catalyzed Fenton reaction.

Bacteria living in air rely on defense systems that detoxify reactive oxygen species, such as superoxide, hydrogen peroxide, and hydroxyl radical, which are generated from incomplete reduction of oxygen by enzymatic and nonenzymatic means. These defense systems include (i) enzymes that scavenge reactive oxygen, such as superoxide dismutases (SOD), catalases, and peroxidases (46); (ii) DNA repair enzymes, such as exonuclease III, DNA polymerase, and RecA (46, 50); (iii) protein repair systems, such as thioredoxin and methionine sulfoxide reductase (15a); and (iv) proteins which regulate the cellular metabolism of iron to ameliorate the generation of reactive oxygen species (46, 50).

Lactic acid bacteria, including *Streptococcus mutans*, cannot synthesize heme and therefore lack catalase and cytochrome oxidases required for energy-linked oxygen metabolism. The growth of lactic acid bacteria, therefore, depends strictly on fermentation. Accordingly, the lactic acid bacteria are considered to have a preference for anaerobiosis. However, many lactic acid bacteria can grow in the presence of oxygen and even consume molecular oxygen through the action of flavoenzymes, such as NADH oxidase, pyruvate oxidase, and α-glycerophosphate oxidase (3, 14, 19, 20, 21, 42). Several antioxidant enzymes, including manganese SOD (13, 33, 38, 41) and none-heme peroxidases, such as manganese-containing catalase (26, 27) and NADH peroxidase (40), which may function as substitutes for catalase, were identified and characterized in lactic acid bacteria. Previously, we identified two components of an NADH-dependent peroxidase (AhpC and Nox-1) from *S. mutans* (20, 21, 36). While studying an *ahpC* and *nox-1* double-disruption mutant of *S. mutans*, we found that the mutant still showed the same level of peroxide tolerance as did the wild-type strain, suggesting the existence of one or more other antioxidants in *S. mutans* (20). In a preceding paper, we identified a *dpr* (for Dps [DNA binding protein from starved cells] [1]-like peroxide resistance gene) gene as a potential peroxide resistance gene from chromosomal DNA of *S. mutans* and demonstrated a functional significance for the gene against oxidative stress (55). The *dpr* disruption mutant of *S. mutans* could not form colonies on agar plates under air. In addition, although *dpr* disruption alone did not interfere with growth in liquid cultures, neither the Δ*dpr* Δ*ahpC* Δ*nox-1* triple mutant nor the Δ*dpr* Δ*sod* double mutant of *S. mutans* was able to grow aerobically in liquid medium. The synthesis of the 20-kDa *dpr* gene product, Dpr, was found to be induced by exposure of *S. mutans* cells to air. Analysis of deduced primary and secondary structures of Dpr suggested that Dpr is a member of the Dps family of proteins (55). Dps is a nonspecific DNA binding protein which accumulates in stationary-phase cells of *Escherichia coli* (1). Members of the Dps family of proteins form spherical complexes, like ferritin, which are composed of 7 to 12 identical subunits of 16 to 22 kDa, and some of them bind iron (1, 6, 15, 22, 34, 48). To date, three family members, including *E. coli* Dps, have been shown to bind to DNA for protection from oxidative stress (1, 8, 34). On the other hand, functional divergence of other Dps family proteins was also reported, i.e., the nonheme ferritin of *Listeria innocua* (6), the fine-tangled-pilus major subunit of *Haemophilus ducreyi* (7), the neutrophil-activating protein (HP-NAP) of *Helicobacter pylori* (48), and a cold shock protein from *Listeria monocytogenes* (18). In this study, we purified Dpr from *S. mutans* and examined its molecular properties to understand how Dpr confers oxygen tolerance on *S. mutans*.

* Corresponding author. Mailing address: Laboratory of Applied Microbiology, Department of Molecular and Cell Biology, Graduate School of Agricultural Science, Tohoku University, 1-1 Tsutsumi-dori, Amamiya-machi, Aoba-ku, Sendai 981-8555, Japan. Phone: 81-22-717-8779. Fax: 81-22-717-8780. E-mail: ykamio@biochem.tohoku.ac.jp.

MATERIALS AND METHODS

Reagents. Horse spleen ferritin, apo-horse spleen ferritin (apoferritin), and 3-(2-pyridyl)-5,6-bis(2-[5-furyl sulfonic acid])-1,2,4-triazine (Ferene S) were purchased from Sigma Chemical Co. (St. Louis, Mo.). Deferoxamine methylate (deferoxamine) was from ICN Pharmaceuticals, K. K., Tokyo, Japan. Bovine serum albumin (BSA), bovine liver catalase, ferrous ammonium sulfate, zinc chloride hexahydrate, 2-deoxyribose, xanthine, xanthine oxidase, and cytochrome *c* were from Wako Pure Chemicals, Osaka, Japan. All other chemicals used were of the best grade commercially available. The stock 100 mM ferrous ammonium sulfate solution in 0.05 N HCl was prepared immediately before use. Apoferritin was further purified by high-performance liquid chromatography (HPLC) with a Mono-Q HR 5/5 column (Amersham Pharmacia Biotech, Tokyo, Japan) using a linear NaCl gradient (0.2 to 0.6 M) in 20 mM Tris-HCl (pH 7.0) because of contamination of SOD activity in the preparation. The purified apoferritin preparation was dialyzed against 0.1 mM MOPS-NaOH (pH 7.0) and concentrated by a CM-50 Centricon ultrafiltration unit (Millipore, Tokyo, Japan) and was used for assays.

Bacterial strains, media, and culture conditions. *S. mutans* GS-5 (53) was routinely grown in TYG medium at 37°C as described previously (55).

Preparation and purification of Dpr. A preculture of 24 ml of *S. mutans* under atmosphere without shaking was used as the inoculum for 2.4 liters of aerobic culture. The cells were incubated for 13 h with vigorous shaking (120 cycles/min), the culture was centrifuged at 12,000 × *g* for 10 min, and the pelleted cells were washed with 100 mM potassium phosphate buffer (pH 7.0) containing 0.5 mM EDTA (buffer A). About 10 g (wet weight) of the cells obtained from 2.4 liters of culture was resuspended in 30 ml of buffer A and disrupted by a French pressure cell. Cell debris was removed by centrifugation at 28,000 × *g* for 30 min, and the supernatant was dialyzed against 20 mM potassium phosphate buffer (pH 7.0) containing 0.5 mM EDTA (buffer B). The dialysate was treated with streptomycin sulfate at a final concentration of 1% (wt/vol) at room temperature for 30 min and centrifuged (28,000 × *g*). The supernatant obtained (about 30 ml) was dialyzed against 80 mM potassium phosphate buffer (pH 7.0) containing 0.5 mM EDTA (buffer C). Sixteen grams of hydroxylapatite powder (Wako Pure Chemicals, Osaka, Japan) was added to the dialysate and kept for 2 h at 4°C with stirring. The hydroxylapatite was recovered, packed in a glass column, and washed with buffer C. The Dpr fraction, which was eluted with 0.2 M potassium phosphate buffer (pH 7.0) containing 0.5 mM EDTA, was dialyzed against a 10-fold volume of distilled water. The dialysate was then subjected to HPLC on a Mono-Q HR 5/5 anion-exchange column using a linear NaCl gradient (0.15 to 0.45 M) in buffer B. The Dpr fraction, which eluted at 0.3 M NaCl, was then subjected to HPLC on an HA-1000 column (Tosoh, Tokyo, Japan) using a linear potassium phosphate gradient (20 to 180 mM) in buffer B. The Dpr fraction, which eluted at 80 mM potassium phosphate, was subjected to HPLC on a DEAE-5PW column (Tosoh) using a linear NaCl gradient (0.1 to 0.3 M) in buffer B. The purity of the Dpr fraction obtained during various steps of the procedure was checked by SDS-PAGE by the method of Laemmli (28), followed by staining with Coomassie brilliant blue R250. The protein concentration was measured by the method of Lowry et al. (30).

Preparation of apo-Dpr. Apo-Dpr was prepared by dialyzing the Dpr preparation against 100 volumes of 20 mM MOPS (morpholinepropanesulfonic acid)-NaOH buffer (pH 7.0) containing 1 mM 2,2′-dipyridyl and 0.3% sodium dithionite at 4°C. The dialysis buffer was changed twice over 36 h. The apo-Dpr preparation was dialyzed against 0.1 mM MOPS-NaOH (pH 7.0) and concentrated (14 to 94 μM) by a CM-50 Centricon and was used for all assays. The apo-Dpr preparation contained <1 atom of iron per molecule of Dpr (see below).

Preparation of iron-loaded Dpr. The iron-loaded Dpr preparation was obtained by incubating 100 μg of the apo-Dpr preparation/ml with 1 mM ferrous ammonium sulfate in 20 mM potassium phosphate buffer (pH 7.0) at room temperature for 1 h. To remove excess iron, the mixture was applied on a DEAE Toyopal 650 M column (Tosoh). The iron-loaded Dpr fraction was eluted with 20 mM potassium phosphate buffer (pH 7.0) containing 0.4 M NaCl. The iron content of the iron-loaded Dpr preparation was determined by atomic absorption spectrometry (170-30; Hitachi, Tokyo, Japan).

The native Dpr and iron-loaded Dpr preparations were also dialyzed against 0.1 mM MOPS-NaOH (pH 7.0), concentrated by a CM-50 Centricon, and used for all assays.

Purification of *E. coli* Dps. For expression of Dps, a DNA fragment containing the *dps* structural gene was amplified from chromosomal DNA of *E. coli* DH-5α by PCR using the primers AGTACCGCTAAATTAGTTAAATCAAAAG (dps2) and AGCGGGATCCTTATTCGATGTTAGACTCGATAAACC (dps3). In dps3, the double underlining indicates the *Bam*HI site. The amplified fragment was digested with *Bam*HI and inserted into the *Nco*I-*Bam*HI site of an expression vector, pTrc99A (Amersham Pharmacia Biotech), to construct plasmid pTRCDPS. Then, *E. coli* DH5α was transformed with pTRCDPS. Purification of *E. coli* Dps from the crude extract of *E. coli* DH5α(pTRCDPS) was done as described by Almiron et al. except that an SP-5PW column (Tosoh) was used for the final step of purification. The purified Dps was dialyzed against 50 mM Tris-HCl (pH 8.0) containing 100 mM NaCl and 1 mM EDTA and then concentrated by a CM-50 Centricon.

Immunoblot analysis. For immunoblot analysis, proteins on SDS-PAGE gels were electrophoretically transferred to polyvinylidene difluoride membranes (Millipore). The membranes were immunostained with a 10,000-fold dilution of an anti-Dpr antiserum which was prepared from a rabbit immunized with the purified Dpr preparation. The reactive proteins were detected using a goat anti-rabbit antibody conjugated to alkaline phosphatase. The Dpr band was developed with nitroblue tetrazolium and 5-bromo-4-chloro-3-indolyl phosphate as the substrate. The amount of Dpr in the cell extract was determined by quantitative comparisons with the signal generated by amounts of the purified Dpr preparation.

Analytical procedures. (i) N-terminal amino acid sequence. The protein on the SDS-polyacrylamide gel was blotted onto a polyvinylidene difluoride membrane, and its N-terminal amino acid sequence was determined by a gas phase protein sequencer (model ABI 491; Applied Biosystems) equipped with an on-line amino acid analyzer (model 610A; Applied Biosystems).

(ii) Metal content in Dpr preparations. The metal contents of native and apo-Dpr preparations were measured by a magnetic sector inductively coupled plasma (ICP) mass spectrometer (ELEMENT; Finnigan MAT) in medium-resolution mode.

(iii) Analytical ultracentrifugation and light-scattering methods. Sedimentation equilibrium analysis was performed using an Optima XL-A analytical ultracentrifuge (Beckman Instruments, Palo Alto, Calif.) essentially as described previously (37). Purified Dpr was concentrated and rediluted three times into 25 mM potassium phosphate buffer with 1 mM EDTA and 0.15 M NaCl at pH 7.0 using CM-10 Centricon ultrafiltration units. Three concentrations of Dpr (4.4 to 38 μM) were loaded (110 μl each) into three of the six sectors of the cell, and buffer from the filtrate was placed in the reference sectors. Data were collected following equilibration at each speed for 12, 14, and 16 h at 20°C. Global analysis of 10 data sets equilibrated at 5,000, 6,500, 9,000, and 12,000 rpm was performed using the Windows version of NONLIN (24). Only data of less than 1.4 absorbance units were used in the analysis. A value of 0.73466 cm^3/g was calculated for the partial specific volume of Dpr from the amino acid composition (29). The buffer density at 1.0077 g/cm^3 was measured using a DA-310 precision density meter (Mettler Toledo, Hightstown, N.J.).

Sedimentation velocity experiments were also carried out at 20°C using three samples and the same buffer described above in double-sectored cells at 0.33, 0.68, and 1.05 starting A_{280} values. Sedimentation data were collected every 4 min at a rotor speed of 35,000 rpm and a radial step size of 0.003 cm. From these data, sedimentation coefficient values at each concentration were calculated using the SVEDBERG program (version 6.23; from J. Philo [http://www.jphilo.mailway.com]) standardized to pure water (corrected for density and viscosity) (29) and were extrapolated to zero concentration to give a value for $s^0_{20,w}$ of 1.241×10^{-12} s. The molecular weight of Dpr was calculated from the Svedberg equation (51) using this $s^0_{20,w}$ value and the corrected translational diffusion coefficient ($D^0_{20,w}$), which was obtained by dynamic light-scattering analysis (see below).

Light-scattering data were acquired using a BI-2030AT correlator operated together with a BI-200SM light-scattering goniometer–photon-counting detector (Brookhaven Instruments, Holtsville, N.Y.) and a model 127 helium-neon laser (35 mW; equipped with a vertical polarization rotator; Spectra Physics, Mountain View, Conn.). For determination of the molecular weight of Dpr by static light-scattering analyses, measurements were made at an angle of 90° in specially formulated microcuvettes (Hellma Cells, Inc.) maintained at 20°C in a refractive-index matching bath (containing 50% glycerol). Samples in the 25 mM potassium phosphate buffer without NaCl were passed through a 0.2-μm-pore-size filter, and the filtrate was collected in acid-washed, dust-free microcuvettes. Sample scattering intensities were corrected for solvent scattering and were expressed relative to a benzene standard (17). Dpr concentrations were measured using the microbiuret protein assay with BSA as a standard (4). A total of 14 intensity measurements from three concentrations of Dpr (0.38 to 1.72 mg/ml) were averaged and used for molecular weight calculations. Weight average molecular weights were determined from the solvent-corrected relative scattering intensity using Rayleigh-Gans-Debye theory (23) and a protein refractive-index increment (dn/dc) of 0.183 ml/g calculated from the amino acid composition (43). Dynamic light scattering was also carried out with the above-mentioned samples to determine the translational diffusion coefficient using the method of cumulants as

described previously (17), and the corrected $D^0_{20,w}$ (51), at $(3.97 \pm 0.42) \times 10^{-7}$ cm^2/s, was used with the sedimentation coefficient to compute a third, independent value for the molecular weight of Dpr.

(iv) Iron and zinc incorporation. For electrophoresis, the apo-Dpr preparation (200 μg/ml) was incubated with 500 μM ferrous ammonium sulfate in 20 mM potassium phosphate (pH 7.0) at room temperature for 1 h. The reaction mixture was subjected to native PAGE, and the protein band containing iron on the gel was detected by Ferene S as described previously (9, 55). To examine the capacity of Dpr to incorporate iron and zinc, 100 μg of the apo-Dpr preparation/ml was incubated with 150 to 500 μM ferrous ammonium sulfate or 50 to 200 μM zinc chloride hexahydrate in 20 mM MOPS-NaOH buffer (pH 7.0) at room temperature for 30 min. Iron- or zinc-loaded Dpr was then purified on a PD-10 column (Amersham Pharmacia Biotech) which was equilibrated with 50 mM MOPS-NaOH buffer (pH 7.0), and the iron and zinc contents of Dpr were determined using an atomic absorption spectrometer. The results shown are means for triplicates.

(v) DNA binding assay. The DNA binding assay was done as described by Almiron et al., who reported that when Dps bound to DNA, the Dps-DNA complex did not enter an agarose gel during electrophoresis (1). According to the method, 5, 10, and 30 μg of the purified or iron-loaded Dpr preparation was added to 200 ng of pUC118, λ DNA, or *S. mutans* genomic DNA in TE (10 mM Tris-HCl, 1 mM EDTA, pH 8.0) and incubated at 37°C for 30 min. The reaction mixture was then electrophoresed through a 1% Tris-acetate agarose gel. DNA on the gel was detected by staining it with ethidium bromide. *E. coli* Dps was used as a positive control.

A DNA-cellulose (Sigma) column, which was equilibrated with 50 mM Tris-HCl (pH 8.0) containing 50 mM NaCl and 1 mM EDTA, was also used to examine the DNA binding ability of Dpr. Both the purified and iron-loaded Dpr preparations were recovered in the flowthrough fraction. In contrast, Dps was eluted at ~0.2 M NaCl by using a linear gradient of 50 to 500 mM NaCl.

(vi) Measurement of SOD and catalase activities. The activity of SOD was measured by the xanthine oxidase-cytochrome *c* method (32). One unit of SOD activity was defined as the amount of protein that gave a 50% decrease in the rate of reduction of cytochrome *c*. Catalase activity was measured according to the method of Beer and Siezer (5). For both assays, 10 to 100 μg of the purified Dpr preparation/ml was used.

(vii) Assay of iron-dependent hydroxyl radical formation. Assay of iron-dependent hydroxyl radical formation was done by the method described by Halliwell and Gutteridge (16). Iron(II) salt in solution generates hydroxyl radical by the following nonenzymatic reactions (16):

$$Fe^{2+} + O_2 \leftrightarrow Fe^{3+} + O_2^- \quad (1)$$

$$2O_2^- + 2H^+ \rightarrow H_2O_2 + O_2 \quad (2)$$

$$H_2O_2 + Fe^{2+} \rightarrow {}^{\cdot}OH + OH^- + Fe^{3+} \quad (3)$$

Hydroxyl radical degrades deoxyribose to a malondialdehyde-like compound which forms a chromogen with thiobarbituric acid. Fluorescence of the chromogen was used as the assay for hydroxyl radical.

The basal reaction mixture contained 10 mM potassium phosphate buffer (pH 7.4), 63 mM NaCl, and 4 mM 2-deoxyribose in a total volume of 0.3 ml. To the basal reaction mixture was added an appropriate amount of Dpr, apoferritin, BSA, deferoxamine, or catalase. The reaction was started by adding ferrous ammonium sulfate to the reaction mixture at a final concentration of 10 μM. After incubation at 37°C for 15 min, 0.25 ml of 1% (wt/vol) thiobarbituric acid and 2.8% (wt/vol) trichloroacetic acid were added to the reaction mixture. After the mixture was boiled for 10 min and rapidly cooled, the amount of chromogen formed in the sample was measured by its fluorescence emission at 553 nm using a Hitachi model 204A fluorescence spectrophotometer (λ_{ex} = 532 nm).

Electron microscopy. Approximately 10 μl of iron-loaded Dpr (50 μg/ml) or horse spleen ferritin (50 μg/ml) in 20 mM MOPS-NaOH (pH 7.0) was placed on carbon-coated grids and negatively stained with 1% (wt/vol) sodium phosphotungstic acid (pH 7.4). The samples were examined under an electron microscope (H-8100; Hitachi) at an acceleration voltage of 100 kV.

Homology search. The amino acid sequences of *S. mutans* Dpr (AB036428), *E. coli* nonheme ferritin (S14069), and *E. coli* bacterioferritin (AF058450.1) were compared with the sequence databases using the BLAST (version 1.49) programs implemented at the EMBL/GenBank/DDBJ, SWISSPROT/NBRF-PIR, and *Streptococcus thermophilus* Sequencing Group at the Catholic University of Louvain (http://www.biol.ucl.ac.be/gene/genome/) and the Microbial Genome Database available through the National Center for Biotechnology Information server (http://www.ncbi.nlm.nih.gov/Microb_blast/unfinishedgenome.html), including *Streptococcus pyogenes*, *Streptococcus pneumoniae*, *S. mutans*, *Streptococcus equi*, *Streptococcus gordonii*, *Enterococcus faecalis*, and *Lactococcus lactis*.

RESULTS

Purification of Dpr from *S. mutans*. We previously identified the *dpr* gene product, Dpr, as a 20-kDa protein in the cell extract of *S. mutans* (55). Dpr was purified to an electrophoretically homogeneous state (Fig. 1A) from crude extracts of *S. mutans* cells, which were grown aerobically, by successive column chromatography using hydroxylapatite, Mono-Q HR 5/5, HA-1000, and DEAE-5PW as described in Materials and Methods. The purified Dpr preparation gave a single absorption maximum at 280 nm and an $A_{280/260}$ value of 1.5 ± 0.02, suggesting that the purified Dpr preparation was free from nucleic acid (10). The N-terminal seven residues of the purified 20-kDa protein were identical to the second through the eighth residues of the deduced amino acid sequence of Dpr. The yield and purification of Dpr were 25.4% and 43.5-fold, respectively, and 2.4 mg of the purified Dpr preparation was obtained from 2.4 liters of culture.

Oligomeric structure of Dpr. Molecular weight determinations were made by three independent methods to determine the subunit composition of Dpr in solution. Sedimentation equilibrium analyses of data sets at a variety of concentrations and speeds yielded molecular weights that exhibited no significant dependence on either protein concentration or rotor speed, consistent with the single-ideal-species model (Fig. 2). Global fits of the data to this model resulted in a weight average molecular weight of 223,000 ± 7,000. Another method for analyzing shape-independent molecular weights of macromolecules, static light scattering, gave an average value of 291,000 ± 22,000 for the molecular weight of Dpr. Finally, using $s^0_{20,w}$ determined from sedimentation velocity measurements and $D^0_{20,w}$ from dynamic light-scattering analyses, the molecular weight of Dpr as calculated from the Svedberg equation (51) is 292,000. The theoretical molecular weight of a single subunit of Dpr, given its lack of the initiating methionine residue, is 19,485.8 g/mol. These data, in combination, are consistent with a subunit composition of 11.5 to 15.0 subunits per molecule.

The dimensions of the Dpr oligomer were also studied by electron microscopy. Negatively stained electron microscopy of Dpr showed ferritin-like spherical structures, which are characteristic of Dps family proteins (Fig. 3). The average diameter of Dpr was calculated to be 9.2 nm, using horse spleen ferritin (12.5-nm diameter) as a standard. The value was similar to that of other Dps family proteins (9.0 to 10.14 nm) (1, 6, 8, 48) but smaller than that of eucaryotic and other bacterial ferritins (11.8 to 13.0 nm) (2).

Iron-binding activity of Dpr. Some Dps family proteins, i.e., ferritin from *L. innocua* and HP-NAP from *H. pylori*, were shown to bind iron (6, 48). Previously, we also detected Dpr as an iron-binding protein from the crude extract of *S. mutans* cells by staining proteins on the polyacrylamide gel with Ferene S (55). In this study, the iron-binding ability of the purified Dpr preparation was examined. As shown in Fig. 1B, both native and iron-loaded Dpr preparations were visualized upon being stained by Ferene S (Fig. 1B, lanes 1 and 3). However, the apo-Dpr preparation was not stained

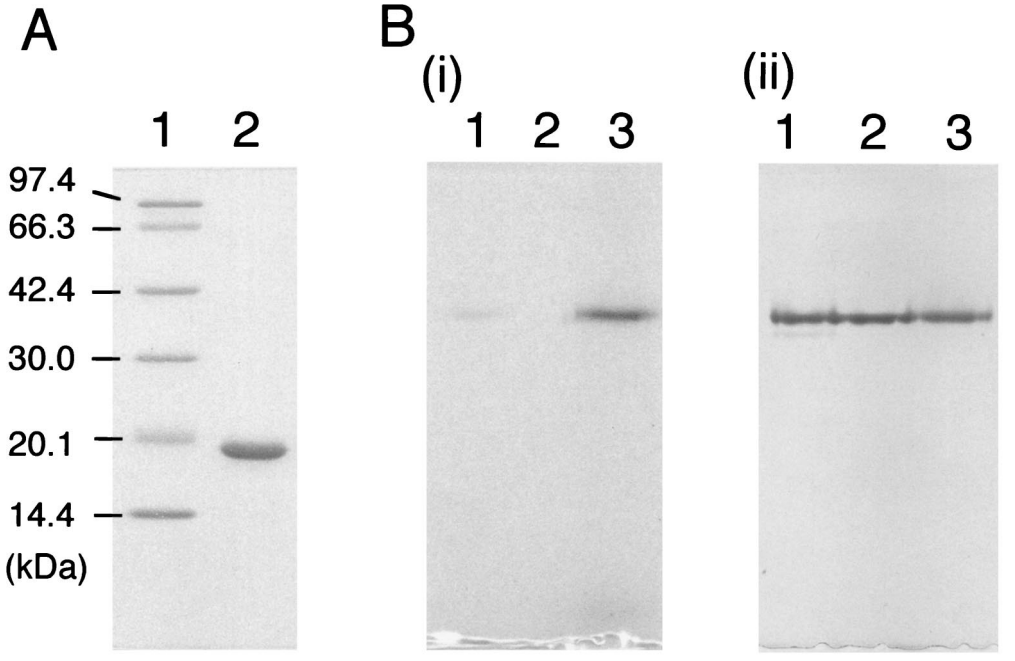

FIG. 1. SDS-PAGE profile for the purified Dpr preparation (A) and its iron-binding activity (B). (A) Molecular weight markers (lane 1) and 2 μg of purified protein (lane 2) were electrophoresed on an SDS-polyacrylamide gel (15.0% [wt/vol]), and the protein bands were stained with Coomassie brilliant blue R250. (B) Native Dpr (lanes 1), apo-Dpr (lanes 2), and iron-loaded Dpr (lanes 3) preparations were electrophoresed on nondenaturing polyacrylamide gel (8.0% [wt/vol]) and stained with Ferene S (i) and Coomassie brilliant blue R250 (ii). Each lane contained 3 μg of Dpr.

by Ferene S (Fig. 1B, lane 2). The staining intensity of the iron-loaded Dpr preparation was approximately 10 times higher than that of the native one. These data clearly indicate that Dpr can bind to iron and that the native Dpr preparation contains iron.

Metal content in the purified Dpr preparation and maximum incorporation of metals into Dpr. Metals in the purified Dpr preparation were analyzed by ICP mass spectrometry. It was revealed that native Dpr from five independent preparations contains iron (10.8 to 27.5 atoms per molecule) and zinc (0.1 to 15.9 atoms per molecule). Dpr preparations also contained Cu, Cr, Mn, Co, Ni, and Mo at <1 atom per molecule. One molecule of Dpr is taken here to consist of 12 identical subunits (see below). In contrast to the native Dpr preparation, the apo-Dpr preparation contained <1 atom of metal per molecule examined.

Maximum incorporation of iron into Dpr was examined by adding various concentrations of ferrous ammonium sulfate (150, 200, 250, 300, 400, and 500 μM) to MOPS-NaOH buffer containing 100 μg of the apo-Dpr preparation/ml. At iron concentrations higher than 250 μM, a brown precipitate of iron was formed, indicating that 250 μM iron is a saturation point for the iron-binding capacity of the protein. Apo-Dpr that was loaded with iron at 250 μM was then purified on a PD-10 column, and the iron content of the protein was measured by atomic absorption spectrometry. It was found that the iron-loaded Dpr preparation contained 40.0 ± 2.2 iron atoms per subunit, corresponding to 480 iron atoms per molecule. This value resembles those reported for *L. innocua* ferritin and *H. pylori* HP-NAP (500 atoms per molecule) (6, 48).

The zinc binding ability of Dpr was also examined using the method described above. The apo-Dpr preparation incorporated up to 11.2 ± 1.7 zinc atoms per molecule.

DNA binding activity. *E. coli* Dps nonspecifically binds DNA to form the stable Dps-DNA complex, which is involved in protection of DNA from hydrogen peroxide by sequestration of the DNA (1, 12, 31, 54). DNA binding activities of other Dps family proteins are also considered to be significant factors in protecting cells from oxidative damage (8, 34). Accordingly, the DNA binding activity of Dpr was assayed. Analyses by agarose gel electrophoresis and DNA-cellulose chromatography were carried out to assess the binding of Dpr to DNA. Addition of the purified *E. coli* Dps preparation to plasmid DNA resulted in the formation of a Dps-DNA complex that was retained in the well after electrophoresis (Fig. 4, lanes 3 and 4). In contrast, addition of the purified Dpr preparation did not affect the mobility of plasmid DNA (Fig. 4, lanes 5, 6, and 7). Addition of the purified Dpr preparation also did not affect the mobility of λ DNA or *S. mutans* genomic DNA (data not shown). When an iron-loaded Dpr preparation was used, the same result was obtained (data not shown). In addition, Dpr did not bind to DNA-cellulose, while *E. coli* Dps bound to DNA-cellulose and eluted at a relatively high salt concentration (~0.2 M NaCl). These results indicated that Dpr did not associate with DNA under the conditions used.

Enzyme activity in Dpr preparation. Neither SOD nor catalase activity was detected in the Dpr preparation.

Inhibition of iron-dependent hydroxyl radical formation by Dpr. The results described above suggest that Dpr functions as a ferritin-like iron-binding protein and that the protection of *S. mutans* from oxidative stress by Dpr might be due to seques-

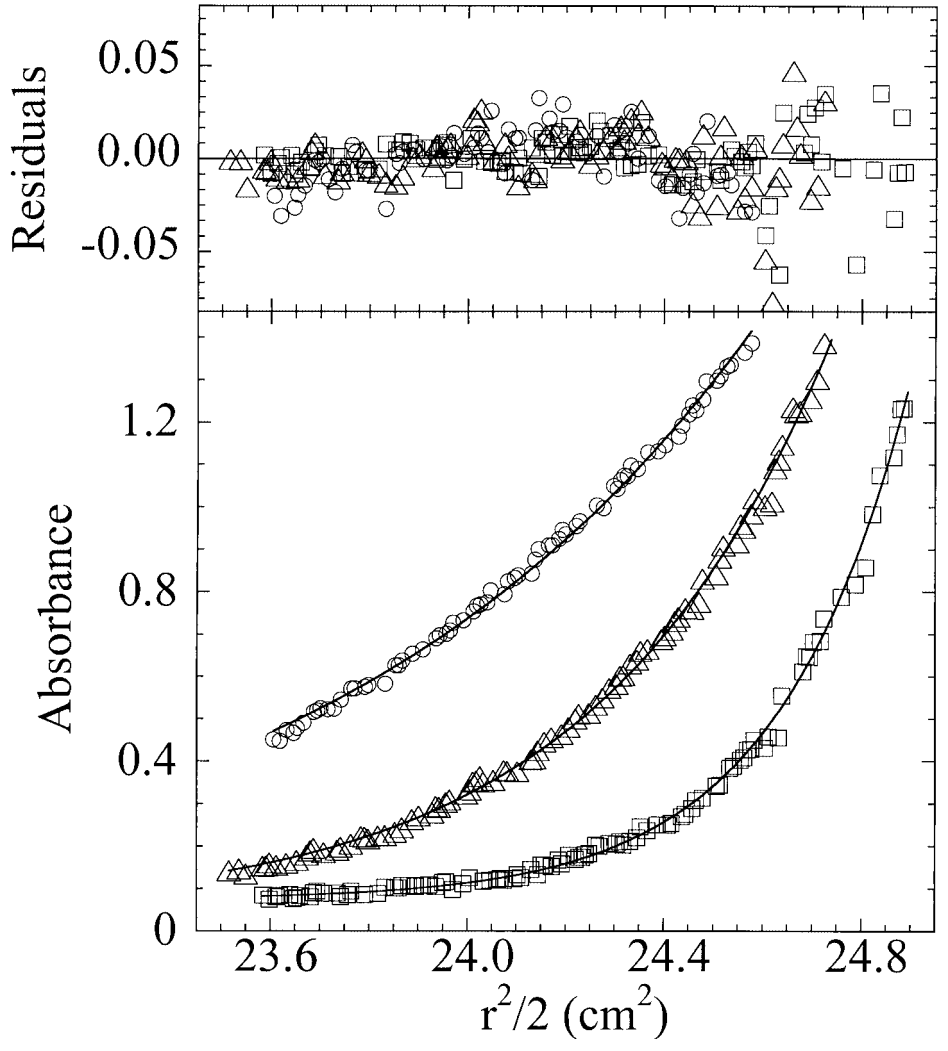

FIG. 2. Sedimentation equilibrium analysis of Dpr to determine molecular weight. Shown are single data sets for 38 μM Dpr equilibrated at 20°C to 6,500 (circles), 9,000 (triangles), and 12,000 (squares) rpm rotor speeds. The solid lines represent global fits to a single ideal species of 14 data sets. The upper panel depicts the deviations between experimental and calculated data (residuals) for each data set. The weight average molecular weight value for Dpr obtained by this method was 239,000 ± 7,000 (variance = 5.62×10^{-4} with 1,066 degrees of freedom) or 223,000 ± 7,000 (variance = 3.64×10^{-4} with 1,056 degrees of freedom) when offset values were floated (25).

tration of iron which otherwise catalyzes the generation of highly toxic radicals, such as hydroxyl radicals. Therefore, the iron-dependent hydroxyl radical formation in the presence or absence of Dpr was investigated as described in Materials and Methods. The results are shown in Table 1. The reaction mixture containing 10 μM iron(II) salt generated hydroxyl radical (see Materials and Methods, reactions 1 to 3) to yield a value of 59.4 fluorescence units (Table 1). Addition of either catalase or deferoxamine, which is an iron chelator, to the reaction mixture caused inhibition of the generation of hydroxyl radical. Addition of apo-Dpr also effectively inhibited hydroxyl radical formation. Seventy-five percent inhibition of hydroxyl radical formation resulted from the addition of 20 nM apo-Dpr at a ratio of apo-Dpr to iron of 1:500. In contrast, 1,000 nM apoferritin inhibited hydroxyl radical formation by only 12.3%. BSA did not inhibit hydroxyl radical formation.

The effect of the iron content of Dpr on the inhibition of hydroxyl radical formation was examined by using preparations of apo-Dpr, native Dpr with 19.8 iron atoms per molecule, and a preparation of iron-loaded Dpr with 277 iron atoms per molecule. As shown in Fig. 5, the extent of the inhibition of hydroxyl radical formation by native Dpr was similar to that by the apo-Dpr preparation, presumably due to the low iron content of the native Dpr preparation. In contrast, the inhibitory capability of the iron-loaded Dpr preparation was significantly decreased but still remained (Fig. 5). These results indicate that the iron-binding ability of Dpr contributes to the inhibition of hydroxyl radical formation and also suggest that the iron-loaded Dpr preparation is still capable of binding iron. A 50% inhibitory concentration value for the inhibition of hydroxyl radical formation, calculated to be 7.5 nM for apo-Dpr, was 6.9-fold lower than that for iron-loaded Dpr (52 nM).

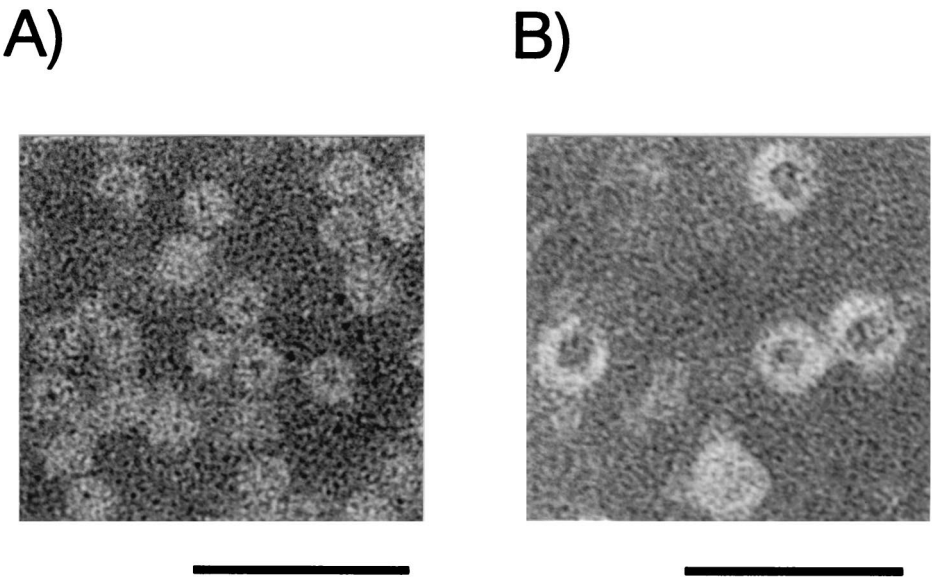

FIG. 3. Electron micrographs of iron-loaded Dpr (A) and horse spleen ferritin (B) preparations. Bars, 45 nm.

DISCUSSION

The *dpr* gene was originally discovered as a potential peroxide tolerance gene in the *S. mutans* chromosome by its ability to complement an alkyl hydroperoxide reductase-deficient mutant of *E. coli* (45) with a *tert*-butyl hydroperoxide-hypersensitive phenotype, and the gene was shown to play an indispensable role in oxygen tolerance in *S. mutans* (55). In this study, we purified Dpr from crude extracts of *S. mutans* and showed, by using electron microscopy and molecular weight determinations of the native Dpr preparation, that Dpr forms spherical oligomers similar to those of other Dps family proteins. The purified Dpr preparation contained a small amount of iron and could incorporate up to 480 iron atoms per molecule. Unlike *E. coli* Dps and two other members of the Dps family (1, 8, 34), Dpr was unable to bind DNA and did not exhibit catalase activity as reported for *Synechococcus* sp. DpsA (35). Thus, a role for Dpr in protection against oxidative stress might involve the sequestration of iron, thereby preventing the generation of highly toxic radicals and conferring oxygen tolerance. As shown in our experiments, Dpr prevented hydroxyl radical formation generated by 10 μM iron(II) salt in vitro (Table 1). This result supported our previous suggestion from the in vivo study that the failure of a series of Dpr-defective mutants to grow under aerobic conditions is caused by the excessive generation of hydroxyl radicals (55). The high intracellular concentration of Dpr determined by Western blotting (~2% of total cellular soluble protein [see Materials and Methods]) might enable cells to be protected from iron-mediated oxidative stress. The contribution of the sequestration of iron by bacterial ferritin to oxidative stress protection was demonstrated in the cases of *Campylobacter jejuni* and an *E. coli fur recA* mutant (49, 52). Recently, intracellular "free-iron" concentrations of *E. coli* and *Saccharomyces cerevisiae* were reported to be 10.0 and 12.8 μM, respectively, using whole-cell electron paramagnetic resonance analyses (25, 44). Though the amount of free iron in *S. mutans* is not known, the observed level of Dpr present in *S. mutans* could prevent hydroxyl radical formation for up to 10.0 μM iron(II). In contrast, apoferritin hardly inhibited hydroxyl radical formation under the conditions shown in Table 1, indicating that under the assay conditions used in this study, there is a competition between nonenzymatic iron oxidation by molecular oxygen (reaction 1) and iron sequestration by Dpr or horse spleen ferritin. Because of this, only an iron-binding protein that can associate with iron faster than it is oxidized could inhibit the reaction. The ability of horse spleen ferritin to incorporate iron [k_{cat} and K_m values for iron(II) → iron(III) are reported to be 80 min^{-1} and 350 μM, respectively (47)] should not be enough to inhibit the reaction, especially for the reaction mixture containing phosphate, which functions as a weak iron chelator and enhances iron oxidation.

Negatively stained protein analyzed by electron microscopy showed ferritin-like spherical structures of Dpr about 9.2 nm in diameter (Fig. 3). Interestingly, the results of dynamic light-scattering analyses to determine the translational diffusion coefficient corresponded to a Stokes radius of 5.5 ± 0.6 nm. This hydrodynamic diameter of about 11.0 nm is in reasonable agreement with the anhydrous diameter from electron microscopy of about 9.2 nm, particularly since the z-average value (23) obtained using the light-scattering method includes bound H_2O molecules and is more sensitive to larger particles. Using three independent methods to assess the molecular weight of Dpr and taking into account its subunit molecular weight, our data also indicate the presence of 11.5 to 15.0 subunits per molecule of Dpr in solution. Given this value and the fact that the iron content of the Dpr preparation used for analysis is approximately 20 atoms per molecule, it is likely that Dpr is a dodecamer in solution. Given an expected molecular weight of 233,830, then, one would predict a translational diffusion coefficient of 5.22×10^{-7} cm^2/s for a solid spherical molecule rather than the measured value of 3.97×10^{-7} cm^2/s, which indicates a larger particle than expected from the molecular

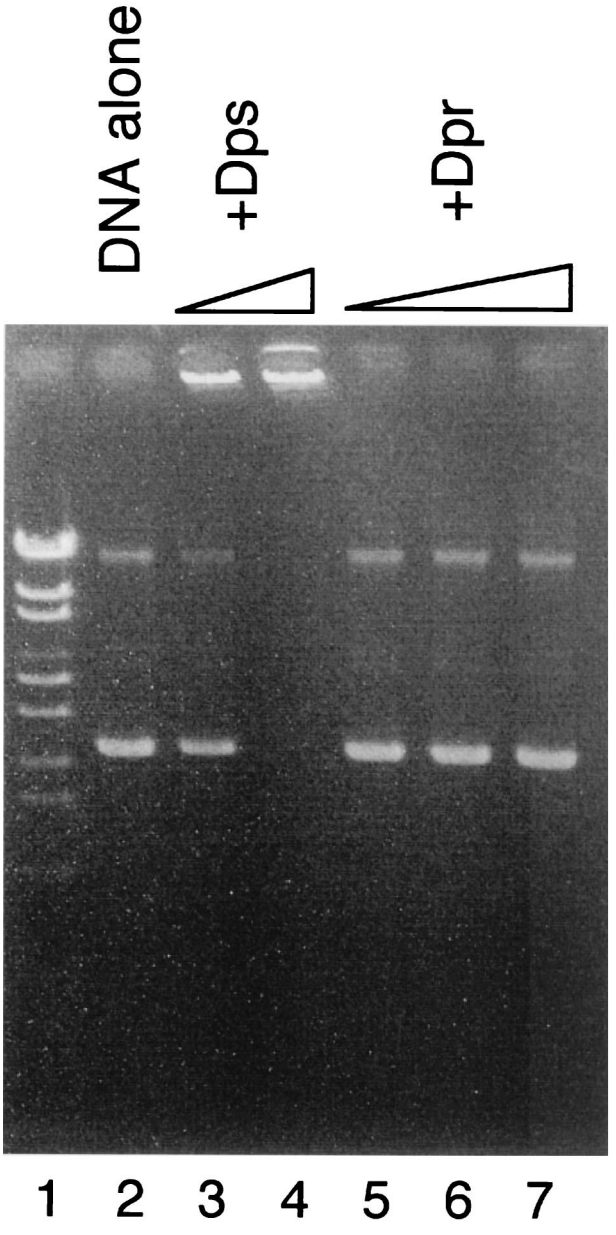

FIG. 4. Assay of DNA binding activity of Dpr. Purified Dps or purified Dpr was added to 200 ng of pUC118 DNA and incubated at 37°C for 30 min. The reaction mixture was then electrophoresed through a 1% Tris-acetate agarose gel. DNA on the gel was detected by staining it with ethidium bromide. Marker DNA (lane 1), pUC118 alone (lane 2), pUC118 with Dps (2.5 and 5.0 μg [lanes 3 and 4]), and pUC118 with Dpr (5.0, 10.0, and 30.0 μg [lanes 5, 6, and 7]) are shown.

weight. This result, together with our electron microscopy data, is consistent with the presence of a cavity in spherical Dpr molecules in which iron atoms can be sequestered, as has been observed previously for ferritins (2).

In bacteria, two types of ferritin molecules, heme-containing bacterioferritin and nonheme ferritin, have been reported (2). Both are composed of 24 identical or similar subunits (2). Recent X-ray crystallographic analyses of two members of the Dps family, *E. coli* Dps and *L. innocua* ferritin, revealed them to be spherical dodecamers consisting of four α-helical bundle

TABLE 1. Effects of Dpr on iron(II)-dependent hydroxyl radical formation[a]

Addition to reaction mixture containing 10 μM iron(II)	Amt	Extent of hydroxyl radical formation (fluorescence emission [arbitrary units])[b]	Inhibition (%)
None		59.4 ± 3.1	
Deferoxamine	10 μM	17.9 ± 4.9	69.9
	100 μM	1.4 ± 0.6	97.6
Catalase	100 U/ml	35.7 ± 4.3	39.9
	1,000 U/ml	11.0 ± 0.9	81.5
Apo-Dpr	20 nM	14.8 ± 0.8	75.1
	100 nM	4.4 ± 0.5	92.6
BSA	1,500 nM	72.8 ± 2.8	<0
	4,500 nM	88.7 ± 3.4	<0
Apoferritin	100 nM	64.0 ± 4.2	<0
	500 nM	60.3 ± 1.3	<0
	1,000 nM	52.1 ± 4.6	12.3

[a] The results are the means ± standard deviations for at least triplicates. Inhibition of hydroxyl radical formation by adding the indicated materials to the reaction mixture is also shown. Data for native and iron-loaded Dpr are shown in Fig. 5 but are not included here for simplicity.
[b] λ_{ex} = 532 nm, λ_{em} = 553 nm.

monomers and also delineated their close structural relationship with other bacterial and eucaryotic ferritin proteins (15, 22). Though the iron-binding ability of *E. coli* Dps is not certain, it is clear that *L. innocua* ferritin, *H. pylori* HP-NAP, and *S. mutans* Dpr all incorporate iron (6, 48). Therefore, at least some members of the Dps protein family, including Dpr, belong to a new class of small ferritins which appear to exist as dodecamers. Dpr was also able to bind zinc ions. Although a physiological role for the zinc binding ability of Dpr is not known, detoxification of zinc by ferritin during overload has been reported (11, 39). To date, ferritin-like proteins have not been reported in lactic acid bacteria, and neither bacteriofer-

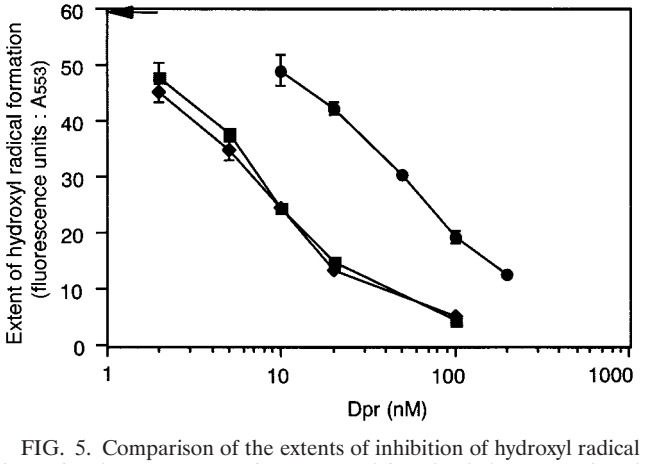

FIG. 5. Comparison of the extents of inhibition of hydroxyl radical formation by apo-Dpr, native Dpr, and iron-loaded Dpr. Hydroxyl radical formation generated by 10 μM ferrous iron in the presence of the indicated amounts of apo-Dpr (squares), native Dpr (diamonds), and iron-loaded Dpr (circles) preparations is shown. Fluorescence data (λ_{ex} = 532 nm; λ_{em} = 553 nm) were obtained following the addition of thiobarbituric acid and trichloroacetic acid as described in Materials and Methods. Without Dpr, a fluorescence value of 59.4 (arrow) was obtained. The results shown are the means and standard deviations for triplicates.

ritin nor nonheme ferritin homologues have been found in genomic sequence data of lactic acid bacteria (see Materials and Methods). In contrast, Dpr and Dps family members were widely distributed among the databases, including *S. pyogenes* (AE006586-6), *S. pneumoniae* (AF055720-1), *Streptococcus thermophilus*, *Streptococcus suis* (AF319974-1), *S. gordonii* (sgord_bvs_203), *E. faecalis* (gef_11370), *L. lactis* (AE006432), *Lactobacillus rhamnosus* (AF037091-2), and *Lactobacillus fermentum* (AB049598-1). Taken together with our results from *S. mutans*, Dps family proteins, as well as Dpr, may act as ferritin in lactic acid bacteria and contribute to the ability of these catalase- and heme-peroxidase-deficient bacteria to grow under air by limiting the iron-catalyzed Fenton reaction.

ACKNOWLEDGMENTS

We are grateful to S. Yamasaki and K. Kimura of Tohoku University for their excellent assistance with ICP mass spectrometry and atomic absorption spectrometry. We also thank T. Sato for his help with the electron microscopy.

This work was supported in part by a Grant-in-Aid for Scientific Research (no. 12876016) from the Japan Society for the Promotion of Sciences (JSPS), the Mishima Kaiun Memorial Foundation, and the Casio Science Promotion Foundation. Y. Yamamoto is the recipient of a predoctoral fellowship from JSPS. Research support to L. B. Poole (NIH RO1 GM50389 and an AHA Established Investigatorship) and R. R. Hantgan (NSF MCB-9728122) is also acknowledged.

REFERENCES

1. **Almiron, M., A. J. Link, D. Furlong, and R. Kolter.** 1992. A novel DNA-binding protein with regulatory and protective roles in starved *Escherichia coli*. Genes Dev. **6:**2646–2654.
2. **Andrews, S. C.** 1998. Iron storage in bacteria. Adv. Microb. Physiol. **40:**281–351.
3. **Auzat, I., S. Chapuy-Regaud, G. Le Bras, D. Dos Santos, A. D. Ogunniyi, I. Le Thomas, J. R. Garel, J. C. Paton, and M. C. Trombe.** 1999. The NADH oxidase of *Streptococcus pneumoniae*: its involvement in competence and virulence. Mol. Microbiol. **34:**1018–1028.
4. **Bailey, J. L.** 1962. Techniques in protein chemistry, p. 294–295. Elsevier Scientific Publishing Co., Inc., New York, N.Y.
5. **Beer, R. F. J., and I. W. Siezer.** 1952. A spectrophotometric method for measuring the breakdown of hydrogen peroxide by catalase. J. Biol. Chem. **195:**276–287.
6. **Bozzi, M., G. Mignogna, S. Stefanini, D. Barra, C. Longhi, P. Valenti, and E. Chiancone.** 1997. A novel non-heme iron-binding ferritin related to the DNA-binding proteins of the Dps family in *Listeria innocua*. J. Biol. Chem. **272:**3259–3265.
7. **Brentjens, R. J., M. Ketterer, M. A. Apicella, and S. M. Spinola.** 1996. Fine tangled pili expressed by *Haemophilus ducreyi* are a novel class of pili. J. Bacteriol. **178:**808–816.
8. **Chen, L., and J. D. Helmann.** 1995. *Bacillus subtilis* MrgA is a Dps (PexB) homologue: evidence for metalloregulation of an oxidative-stress gene. Mol. Microbiol. **18:**295–300.
9. **Chung, M. C.** 1985. A specific iron stain for iron-binding proteins in polyacrylamide gels: application to transferrin and lactoferrin. Anal. Biochem. **148:**498–502.
10. **Copeland, R. A.** 1994. Methods for protein analysis. Chapman and Hall, London, United Kingdom.
11. **Dundon, W. G., A. Polenghi, G. Del Guidice, R. Rappuoli, and C. Montecucco.** 2001. Neutrophil-activating protein (HP-NAP) versus ferritin (Pfr): comparison of synthesis in *Helicobacter pylori*. FEMS Microbiol. Lett. **199:**143–149.
12. **Frenkiel-Krispin, D., S. Levin-Zaidman, E. Shimoni, S. G. Wolf, E. J. Wachtel, T. Arad, S. E. Finkel, R. Kolter, and A. Minsky.** 2001. Regulated phase transitions of bacterial chromatin: a non-enzymatic pathway for generic DNA protection. EMBO J. **20:**1184–1191.
13. **Gibson, C. M., and M. G. Caparon.** 1996. Insertional inactivation of *Streptococcus pyogenes sod* suggests that *prtF* is regulated in response to a superoxide signal. J. Bacteriol. **178:**4688–4695.
14. **Gibson, C. M., T. C. Mallett, A. Claiborne, and M. G. Caparon.** 2000. Contribution of NADH oxidase to aerobic metabolism of *Streptococcus pyogenes*. J. Bacteriol. **182:**448–455.
15. **Grant, R. A., D. J. Filman, S. E. Finkel, R. Kolter, and J. M. Hogle.** 1998. The crystal structure of Dps, a ferritin homolog that binds and protects DNA. Nat. Struct. Biol. **5:**294–303.

15a. **Grimaud, R., B. Ezraty, J. K. Mitchell, D. Lafitte, C. Briand, P. J. Derrick, and F. Barras.** 2001. Repair of oxidized proteins. Identification of a new methionine sulfoxide reductase. J. Biol. Chem. **276:**48915–48920.

16. **Halliwell, B., and J. M. Gutteridge.** 1981. Formation of a thiobarbituric acid reactive substance from deoxyribose in the presence of iron salts. FEBS Lett. **128:**347–352.
17. **Hantgan, R. R., J. V. Braaten, and M. Rocco.** 1993. Dynamic light scattering studies of α_{2b} β_3 solution conformation. Biochemistry **32:**3935–3941.
18. **Hebraud, M., and J. Guzzo.** 2000. The main cold shock protein of *Listeria monocytogenes* belongs to the family of ferritin-like proteins. FEMS Microbiol. Lett. **190:**29–34.
19. **Higuchi, M., M. Shimada, Y. Yamamoto, T. Hayashi, T. Koga, and Y. Kamio.** 1993. Identification of two distinct NADH oxidases corresponding to H_2O_2-forming oxidase and H_2O-forming oxidase induced in *Streptococcus mutans*. J. Gen. Microbiol. **139:**2343–2351.
20. **Higuchi, M., Y. Yamamoto, L. B. Poole, M. Shimada, Y. Sato, N. Takahashi, and Y. Kamio.** 1999. Functions of two types of NADH oxidases in energy metabolism and oxidative stress of *Streptococcus mutans*. J. Bacteriol. **181:**5940–5947.
21. **Higuchi, M., Y. Yamamoto, and Y. Kamio.** 2000. Molecular biology of oxygen tolerance in lactic acid bacteria: functions of NADH oxidases and Dpr in oxidative stress. J. Biosci. Bioeng. **90:**484–493.
22. **Ilari, A., S. Stefanini, E. Chiancone, and D. Tsernoglou.** 2000. The dodecameric ferritin from *Listeria innocua* contains a novel intersubunit iron-binding site. Nat. Struct. Biol. **7:**38–43.
23. **Johnson, C. S., and D. A. Gabriel.** 1981. Laser light scattering, p. 177–272. *In* J. E. Bell (ed.), Spectroscopy in biochemistry, vol. II. CRC Press, Boca Raton, Fla.
24. **Johnson, M., J. J. Correia, D. A. Yphantis, and H. Halvorson.** 1981. Analysis of data from the analytical ultracentrifuge by nonlinear least-squares techniques. Biophys. J. **36:**575–588.
25. **Keyer, K., and J. A. Imlay.** 1996. Superoxide accelerates DNA damage by elevating free-iron levels. Proc. Natl. Acad. Sci. USA **93:**13635–13640.
26. **Kono, Y., and I. Fridovich.** 1983. Isolation and characterization of the pseudocatalase of *Lactobacillus plantarum.* J. Biol. Chem. **258:**6015–6019.
27. **Kono, Y., and I. Fridovich.** 1983. Functional significance of manganese catalase in *Lactobacillus plantarum*. J. Bacteriol. **155:**742–746.
28. **Laemmli, U. K.** 1970. Cleavage of structural proteins during the assembly of the head of bacteriophage T4. Nature **227:**680–685.
29. **Laue, T. M., B. D. Shah, T. M. Ridgeway, and S. L. Pelletier.** 1992. Computer-aided interpretation of analytical sedimentation data for proteins, p. 90–125. *In* S. E. Harding, A. J. Rowe, and J. C. Horton (ed.), Analytical ultracentrifugation in biochemistry and polymer science. The Royal Society of Chemistry, Cambridge, United Kingdom.
30. **Lowry, O. H., N. J. Rosebrough, A. L. Farr, and R. J. Randall.** 1951. Protein measurement with the Folin phenol reagent. J. Biol. Chem. **193:**265–275.
31. **Martinez, A., and R. Kolter.** 1997. Protection of DNA during oxidative stress by the nonspecific DNA-binding protein Dps. J. Bacteriol. **179:**5188–5194.
32. **McCord, J. M., and I. Fridovich.** 1969. Superoxide dismutase. An enzymatic function for erythrocuprein (hemocuprein). J. Biol. Chem. **224:**6049–6055.
33. **Nakayama, K.** 1992. Nucleotide sequence of *Streptococcus mutans* superoxide dismutase gene and isolation of insertion mutants. J. Bacteriol. **174:**4928–4934.
34. **Pena, M. M., W. Burkhart, and G. S. Bullerjahn.** 1995. Purification and characterization of a *Synechococcus* sp. strain PCC 7942 polypeptide structurally similar to the stress-induced Dps/PexB protein of *Escherichia coli*. Arch. Microbiol. **163:**337–344.
35. **Pena, M. M., and G. S. Bullerjahn.** 1995. The DpsA protein of *Synechococcus* sp. strain PCC7942 is a DNA-binding hemoprotein. Linkage of the Dps and bacterioferritin protein families. J. Biol. Chem. **270:**22478–22482.
36. **Poole, L. B., M. Higuchi, M. Shimada, M. L. Calzi, and Y. Kamio.** 2000. *Streptococcus mutans* H_2O_2-forming NADH oxidase is an alkyl hydroperoxide reductase protein. Free. Radic. Biol. Med. **28:**108–120.
37. **Poole, L. B., A. Godzik, A. Nayeem, and J. D. Schmitt.** 2000. AhpF can be dissected into two functional units: tandem repeats of two thioredoxin-like folds in the N-terminus mediate electron transfer from the thioredoxin reductase-like C-terminus to AhpC. Biochemistry **39:**6602–6615.
38. **Poyart, C., E. Pellegrini, O. Gaillot, C. Boumaila, M. Baptista, and P. Trieu-Cuot.** 2001. Contribution of Mn-cofactored superoxide dismutase (SodA) to the virulence of *Streptococcus agalactiae*. Infect. Immun. **69:**5098–5106.
39. **Price, D., and J. G. Joshi.** 1982. Ferritin: a zinc detoxicant and a zinc ion donor. Proc. Natl. Acad. Sci. USA **79:**3116–3119.
40. **Ross, R. P., and A. Claiborne.** 1991. Cloning, sequence and overexpression of NADH peroxidase from *Streptococcus faecalis* 10C1. Structural relationship with the flavoprotein disulfide reductases. J. Mol. Biol. **221:**857–871.
41. **Sanders, J. W., K. J. Leenhouts, A. J. Haandrikman, G. Venema, and J. Kok.** 1995. Stress response in *Lactococcus lactis*: cloning, expression analysis, and mutation of the lactococcal superoxide dismutase gene. J. Bacteriol. **177:**5254–5260.
42. **Schmidt, H. L., W. Stocklein, J. Danzer, P. Kirch, and B. Limbach.** 1986.

Isolation and properties of an H_2O-forming NADH oxidase from *Streptococcus faecalis*. Eur. J. Biochem. **156:**149–155.
43. **Spotorno, B., L. Piccinini, G. Tassara, C. Ruggiero, M. Nardini, F. Molina, and M. Rocco.** 1997. BEAMS (BEAds Modelling System): a set of computer programs for the generation, the visualization and the computation of the hydrodynamic and conformational properties of bead models of proteins. Eur. Biophys. J. **25:**373–384.
44. **Srinivasan, C., A. Liba, J. A. Imlay, J. S. Valentine, and E. B. Gralla.** 2000. Yeast lacking superoxide dismutase(s) show elevated levels of "free iron" as measured by whole cell electron paramagnetic resonance. J. Biol. Chem. **275:**29187–29192.
45. **Storz, G., F. S. Jacobson, L. A. Tartaglia, R. W. Morgan, L. A. Silveira, and B. N. Ames.** 1989. An alkyl hydroperoxide reductase induced by oxidative stress in *Salmonella typhimurium* and *Escherichia coli*: genetic characterization and cloning of *ahp*. J. Bacteriol. **171:**2049–2055.
46. **Storz, G., and J. A. Imlay.** 1999. Oxidative stress. Curr. Opin. Microbiol. **2:**188–194.
47. **Sun, S., and N. D. Chasteen.** 1992. Ferroxidase kinetics of horse spleen apo-ferritin. J. Biol. Chem. **267:**25160–25166.
48. **Tonello, F., W. G. Dundon, B. Satin, M. Molinari, G. Tognon, G. Grandi, G. Del Giudice, R. Rappuoli, and C. Montecucco.** 1999. The *Helicobacter pylori* neutrophil-activating protein is an iron-binding protein with dodecameric structure. Mol. Microbiol. **34:**238–246.
49. **Touati, D., M. Jacques, B. Tardat, L. Bouchard, and S. Despied.** 1995. Lethal oxidative damage and mutagenesis are generated by iron in Δ*fur* mutants of *Escherichia coli*: protective role of superoxide dismutase. J. Bacteriol. **177:** 2305–2314.
50. **Touati, D.** 2000. Iron and oxidative stress in bacteria. Arch. Biochem. Biophys. **373:**1–6.
51. **Van Holde, K. E.** 1971. Physical biochemistry, 2nd ed., p. 110–136. Prentice-Hall, Inc., Englewood Cliffs, N.J.
52. **Wai, S. N., K. Nakayama, K. Umene, T. Moriya, and K. Amako.** 1996. Construction of a ferritin-deficient mutant of *Campylobacter jejuni*: contribution of ferritin to iron storage and protection against oxidative stress. Mol. Microbiol. **20:**1127–1134.
53. **Wetherell, J. R., Jr., and A. S. Bleiweis.** 1975. Antigens of *Streptococcus mutans*: characterization of a polysaccharide antigen from walls of strain GS-5. Infect. Immun. **12:**1341–1348.
54. **Wolf, S. G., D. Frenkiel, T. Arad, S. E. Finkel, R. Kolter, and A. Minsky.** 1999. DNA protection by stress-induced biocrystallization. Nature **400:**83–85.
55. **Yamamoto, Y., M. Higuchi, L. B. Poole, and Y. Kamio.** 2000. Role of the *dpr* product in oxygen tolerance in *Streptococcus mutans*. J. Bacteriol. **182:**3740–3747.